

Blocker Studies of the Functional Architecture of the NMDA Receptor Channel

A. I. Sobolevskii and B. I. Khodorov

Translated from Rossiiskii Fiziologicheskii Zhurnal imeni I. M. Sechenova, Vol. 86, No. 9, pp. 1118–1137, September, 2000. Original article submitted March 7, 2000.

Blockade of ion channels passing through the NMDA receptors of isolated rat hippocampus pyramidal neurons with tetraalkylammonium compounds, 9-aminoacridine, and Mg^{2+} was studied using patch-clamp methods in the whole-cell configuration. Currents through NMDA channels were evoked by application of 100 μM aspartate in magnesium-free medium containing glycine (3 μM) to neurons. Analysis of the kinetics, charge transfer, and relationships between the extent of suppression of stationary currents on the one hand and membrane potential, agonist concentration, and blocker concentration on the other showed that blockers had different effects on the closing, desensitization, and agonist dissociation of NMDA channels. The size of the blocker was found to be the decisive factor determining its action on the gating functions of NMDA channels: larger blockers prevented closure and/or desensitization of the channel; smaller blockers only had partial effects on these processes, while the smallest blockers had no effect at all. These experiments showed that the apparent affinity of the blocker for the channel ($1/IC_{50}$) depended not only on the microscopic equilibrium dissociation constant (K_d), but also on the number of blocker binding sites, their mutual influences, and, of particular importance, the interaction of the blocker with the gating structures of the channel. These data led us to propose hypotheses relating to the geometry of the NMDA channel and the structure of its gating mechanism. The channel diameter at the level of activated gates was estimated to be 11 Å.

KEY WORDS: NMDA channels, gating structures, blockade, kinetic modeling, hippocampal neurons, patch-clamping.

The properties of the NMDA (N-methyl-D-aspartate) subtype of glutamate channels, such as the high permeability for calcium ions [28], potential-dependent magnesium blockade [30], and slow activation kinetics [22, 25] determine their major contribution to physiological processes.

According to current concepts, NMDA channels play a key role in learning and memory processes [8, 12, 29]. Their involvement in generating rhythmic movement activity has been demonstrated [36], along with their role in the development of the nervous system at the embryo stage [13, 14, 24]. Many neurodegenerative processes are associated with hyperactivity of NMDA channels. On this principle, NMDA channel blockers such as memantine (1-amino-3,5-dimethyladamantane) and amantadine (1-adamantanamine) are used in the treatment of Alzheimer's disease, Parkin-

son's disease, Huntingdon's chorea, dyskinesia, sclerosis, allergic encephalomyelitis, epilepsy, depression, ischemia, schizophrenia, hemiplegia, the chronic pains involved in all types of dementia, including AIDS-associated dementia, and paralysis [17, 18, 27, 31, 32].

Recent years have seen significant progress in studies of the molecular structures, subunit composition, and selectivity of NMDA channels [19], though the question of the mechanisms of NMDA channel activation and desensitization has still not been elucidated completely.

The present article summarizes the results of studies conducted by our group in recent years with the aim of identifying the functional architecture of NMDA channels and their gating mechanism. The tools for these studies were organic cations (9-aminoacridine and tetraalkylammonium compounds) and magnesium ions, which can enter open channels and interact in different ways with the structural elements of the channels responsible for activation and desensitization processes [1, 2, 33, 35].

Institute of General Pathology and Pathophysiology, Russian Academy of Medical Sciences, 8 Baltiiskaya Street, 125315 Moscow, Russia.

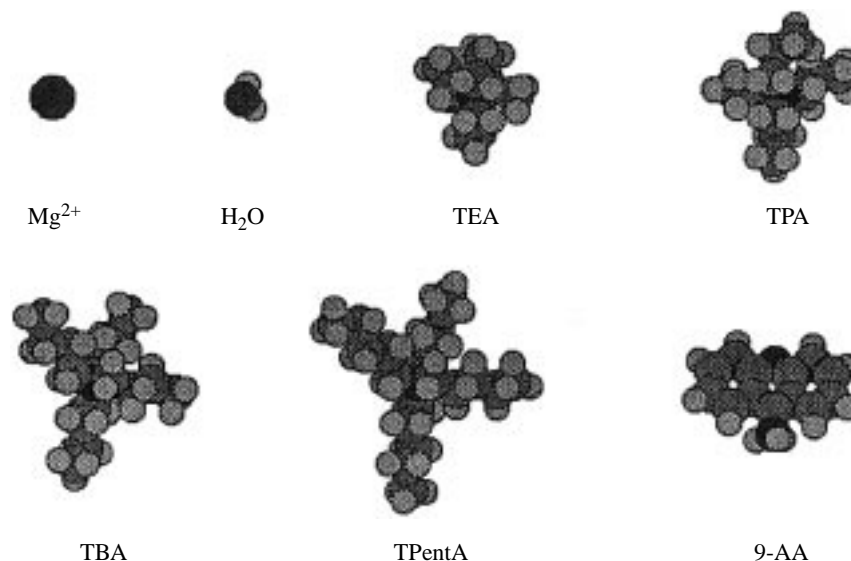


Fig. 1. NMDA channel blockers: Mg^{2+} , water (H_2O), tetraethylammonium (TEA), tetrapropylammonium (TPA), tetrabutylammonium (TBA), tetrapentylammonium (TPentA), and 9-aminoacridine (9-AA). Black circles show nitrogen and magnesium atoms, dark gray circles show carbon and oxygen atoms, and light gray circles show hydrogen atoms.

METHODS

Experiments were performed on pyramidal neurons from field CA1 of the rat hippocampus. Sections were made of brains from Wistar rats aged 2–4 weeks, as described previously [38]. Neurons were extracted from sections using a vibrodissociation method [38]. Experiments were started after at least 3 h of incubation in medium containing 124 mM NaCl, 3 mM KCl, 1.4 mM CaCl_2 , 2 mM MgCl_2 , 10 mM glucose, and 26 mM NaHCO_3 . Incubation was conducted with the solution continuously saturated with gas mix (96% O_2 , 4% CO_2), at a temperature of 32°C. During removal from sections and recording of currents, neurons were kept in magnesium-free medium containing 140 mM NaCl, 5 mM KCl, 2 mM CaCl_2 , 15 mM glucose, and 10 mM HEPES, pH 7.3. All blockers were dissolved in water; solutions were stored in a freezer and were thawed immediately before experiments. A rapid flow control system was used for exchanging solutions [11, 38]. Transmembrane currents in whole cells were recorded by a patch-clamping method at room temperature using micropipettes made of hard borosilicate glass (Pyrex), filled with “intracellular” solution containing 140 mM CsF, 4 mM NaCl, and 10 mM HEPES, pH 7.2. The resistance of filled micropipettes was 3–7 M Ω . Currents were digitized at a frequency of 1 kHz and recorded in a computer memory.

Data were analyzed statistically using Microcal Origin version 3.5 for Windows. Data are presented as means \pm standard errors.

Kinetic modeling was based on the solution of linear systems of first-order differential equations with constant coefficients by numerical methods, as described previously [11].

Three-dimensional models of blocker molecules were calculated using the molecular modeling program HyperChem version 3 for Windows.

RESULTS AND DISCUSSION

Kinetics and Stationary Characteristics of Open NMDA Channel Blockade. Figure 1 shows the NMDA channel blockers used here: Mg^{2+} , tetraethylammonium, tetrapropylammonium, tetrapentylammonium, and 9-aminoacridine, whose effects were studied in the present experiments.

Currents through NMDA channels arose in response to the application of 100 μM aspartate in magnesium-free medium containing glycine (3 μM). At a membrane potential $E_h = -100$ mV, the current was an influx current; after a rapid ($\tau < 30$ msec) increase to a peak value (I_{CO}), it started to decay slowly ($\tau = 570 \pm 25$ msec, $n = 7$) until it reached a certain stationary value (I_{CS}) (Fig. 2, A). This decay in the current in the constant presence of agonist is interpreted as desensitization of NMDA channels. The extent of desensitization ($1 - (I_{\text{CS}}/I_{\text{CO}})$) varied from cell to cell over a wide range, from 0.08 to 0.75.

Used simultaneously with agonist, blockers decreased both the peak (I_{BO}) and stationary (I_{BS}) currents (Fig. 2, A). After coapplication ended, an influx aftercurrent appeared (a “hook”), which quickly reached a peak (I_p) and then decayed to zero. The relative amplitude of the hook $[(I_p - I_{\text{BS}})/I_{\text{CS}}]$ increased with increasing blocker concentrations and, correspondingly, with increases in the degree of suppression of the

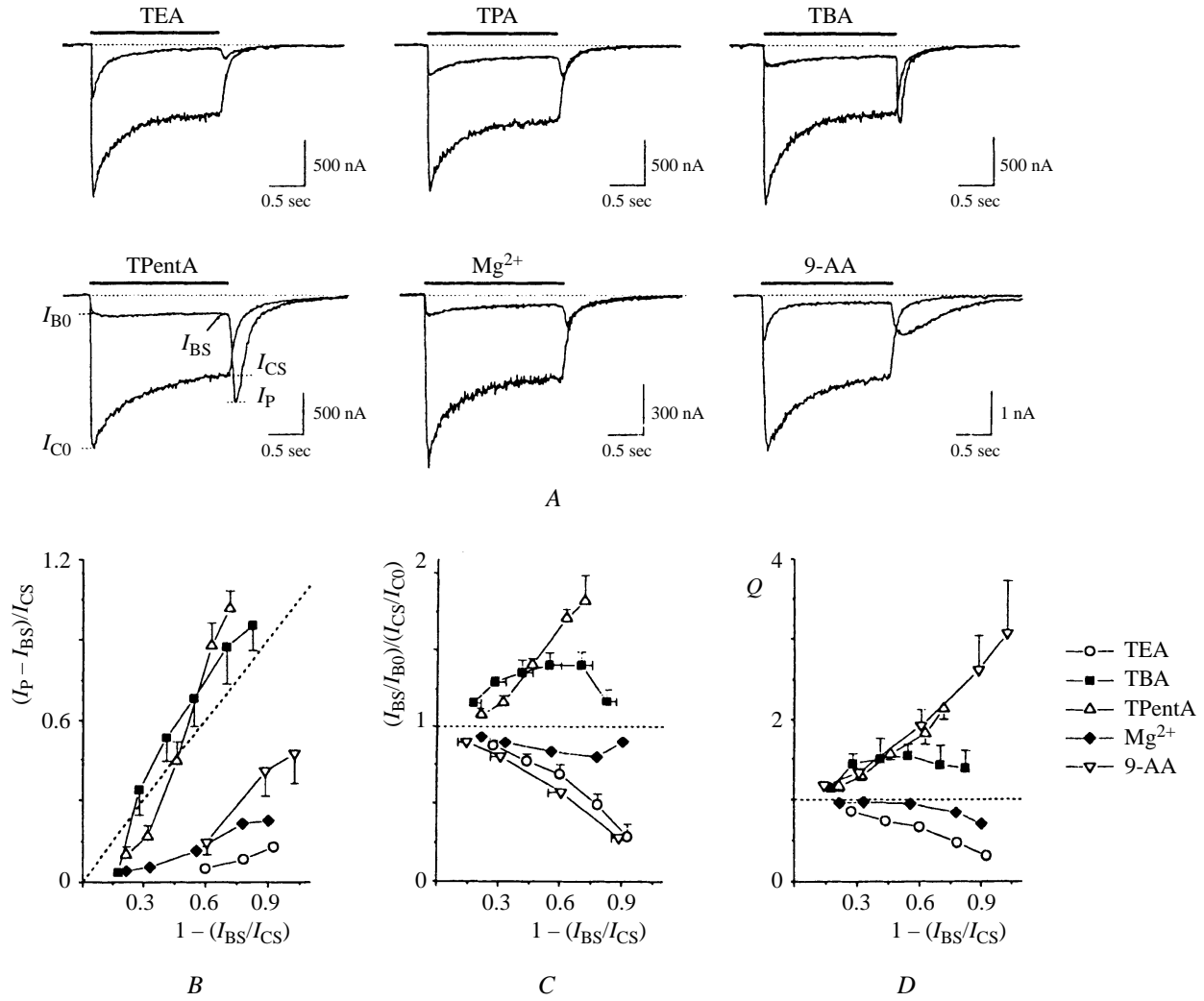


Fig. 2. The effects of simultaneous exposure to blockers and agonist. A) Superimposition of control current in response to application of aspartate (100 μ M) and the blocked current in response to simultaneous application of aspartate and tetraethylammonium (TEA, 10 mM), tetrapropylammonium (TPA, 2 mM), tetrabutylammonium (TBA, 2 mM), tetrapentylammonium (TPentA, 3 mM), Mg^{2+} (100 μ M), and 9-aminoacridine (9-AA, 10 μ M); B, C, D) relationships of the maximum hook amplitude $(I_P - I_{BS})/I_{CS}$ (B), the control-normalized ratio of stationary current to peak current $[(I_{BS}/I_{B0})/(I_{CS}/I_{C0})]$ (C), and the control-normalized charge transfer during the aftercurrent (Q) (D) with the extent of suppression of the stationary current $(1 - (I_{BS}/I_{CS}))$.

TABLE 1. Parameters of Potential Dependence (from [35] with additional data)

Substance	δ	$K_{0.5}(0)$, mm	n
Tetraethylammonium	0.90 ± 0.04	62.2 ± 6.0	6
Tetrapropylammonium	0.72 ± 0.05	10.0 ± 1.5	4
Tetrabutylammonium	0.60 ± 0.02	5.34 ± 0.27	7
Tetrapentylammonium	0.29 ± 0.03	1.84 ± 0.11	5
Mg^{2+}	0.93 ± 0.19	6.57 ± 2.95	11
9-Aminoacridine	0.65 ± 0.05	0.162 ± 0.070	4

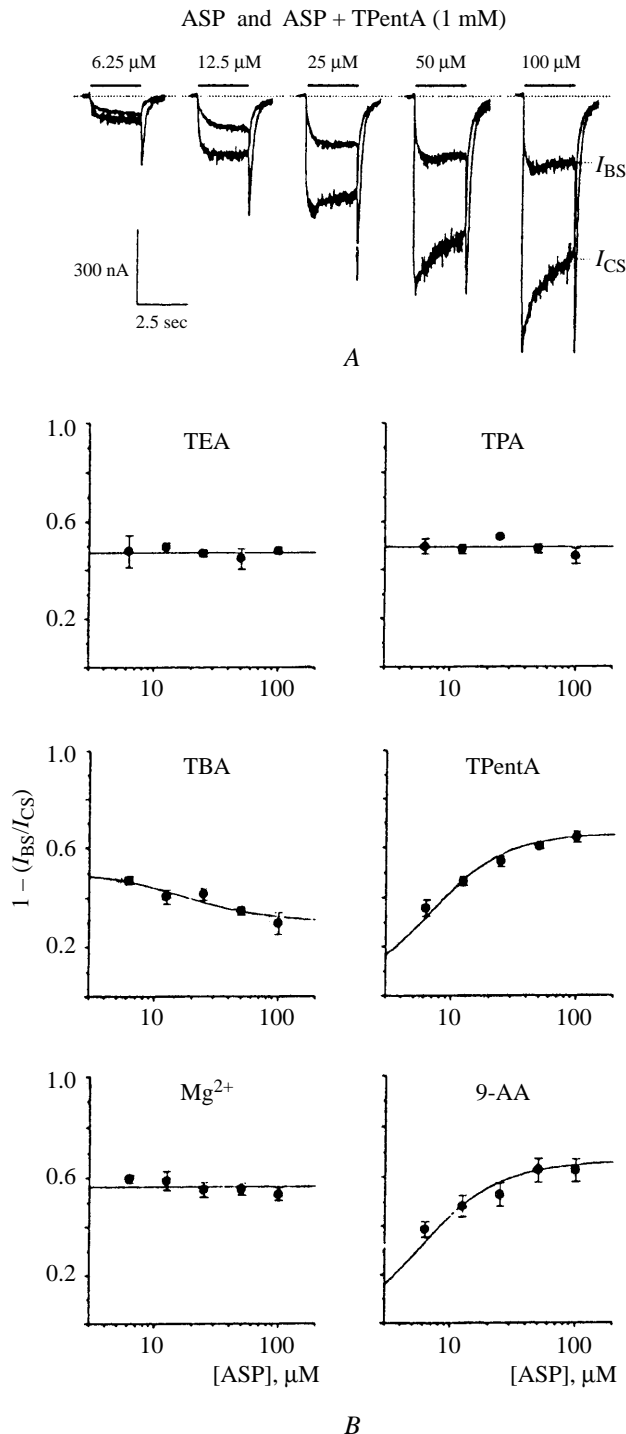


Fig. 3. Agonist-dependent blockade. A) Currents in response to simultaneous use of tetrapentylammonium (TPentA, 1 mM) and aspartate (ASP) at different concentrations superimposed on control traces; B) relationships between mean extents of suppression of the stationary current ($1 - (I_{BS}/I_{CS})$) and the ASP concentration (from [35] with additional data).

stationary current ($1 - (I_{BS}/I_{CS})$) (Fig. 2, B). For Mg^{2+} , tetraethylammonium, tetrapropylammonium, and 9-aminoacridine, $(I_P - I_{BS})/I_{CS}$ was less than $1 - I_{BS}/I_{CS}$, while in the cases of tetrabutylammonium and tetrapentylammonium, especially at high blocker concentrations, $(I_P - I_{BS})/I_{CS}$ was greater than $1 - I_{BS}/I_{CS}$ (in Fig. 2, B, the points lie above the dotted line corresponding to $(I_P - I_{BS})/I_{CS} = 1 - (I_{BS}/I_{CS})$).

Changes in the kinetics of aftercurrents in the presence of different blockers were different. The decay phase of the hook was delayed as compared with decay in the control current when tetrabutylammonium, tetrapentylammonium, and 9-aminoacridine were used (intercepts of aftercurrents in Fig. 2, A); these coincided in the case of Mg^{2+} and tetrapropylammonium, while decay in controls was slightly delayed compared with decay of currents blocked by tetraethylammonium.

The "desensitization" decay in the current during coapplication of aspartate and blockers (I_{BO}/I_{BS}) was smaller than in controls (I_{CO}/I_{CS}) in the presence of tetrabutylammonium and tetrapentylammonium, essentially the same in the presence of tetrapropylammonium and Mg^{2+} , and greater than in controls in the presence of tetraethylammonium and 9-aminoacridine (Fig. 2, A). This is well illustrated by the integral curves of $(I_{BS}/I_{BO})/(I_{CS}/I_{CO})$, which for these blockers were greater than 1, around 1, and less than 1 respectively (Fig. 2, C).

Transfer of charge through NMDA channels, measured by integration of current curves after the end of coapplication of aspartate and blockers, for tetrabutylammonium, tetrapentylammonium, and 9-aminoacridine was greater than charge transfer after the end of exposure to aspartate alone. The ratios of these charges (Q) were greater than 1 and increased with increasing blocker concentration (Fig. 2, D). In the case of Mg^{2+} , tetraethylammonium, and tetrapropylammonium, Q was less than unity and decreased with increasing blocker concentrations (Fig. 2, D).

All blockers decreased the level of suppression of the stationary current ($1 - (I_{BS}/I_{CS})$) with increases in the level of cell membrane depolarization. The relationship between $1 - (I_{BS}/I_{CS})$ and membrane potential (E_h) fit the model [39] described by the following equation:

$$1 - I_{BS}/I_{CS} = 1 - 1/(1 + [B]/K_{0.5}(0) \cdot \exp(\delta FE_h/RT)),$$

where $K_{0.5}(0)$ is the equilibrium dissociation constant at $E_h = 0$ and δ is the proportion of the membrane potential obtaining at the blocker binding site in the channel pore. Smaller blockers penetrated deeper into the channel across the transmembrane field than larger blockers. This is clearly illustrated in Table 1, which give values for δ and $K_{0.5}(0)$ for all blockers.

The degrees of suppression of the stationary current ($1 - (I_{BS}/I_{CS})$) for different blockers showed different relationships with agonist concentration. Figure 3, A shows,

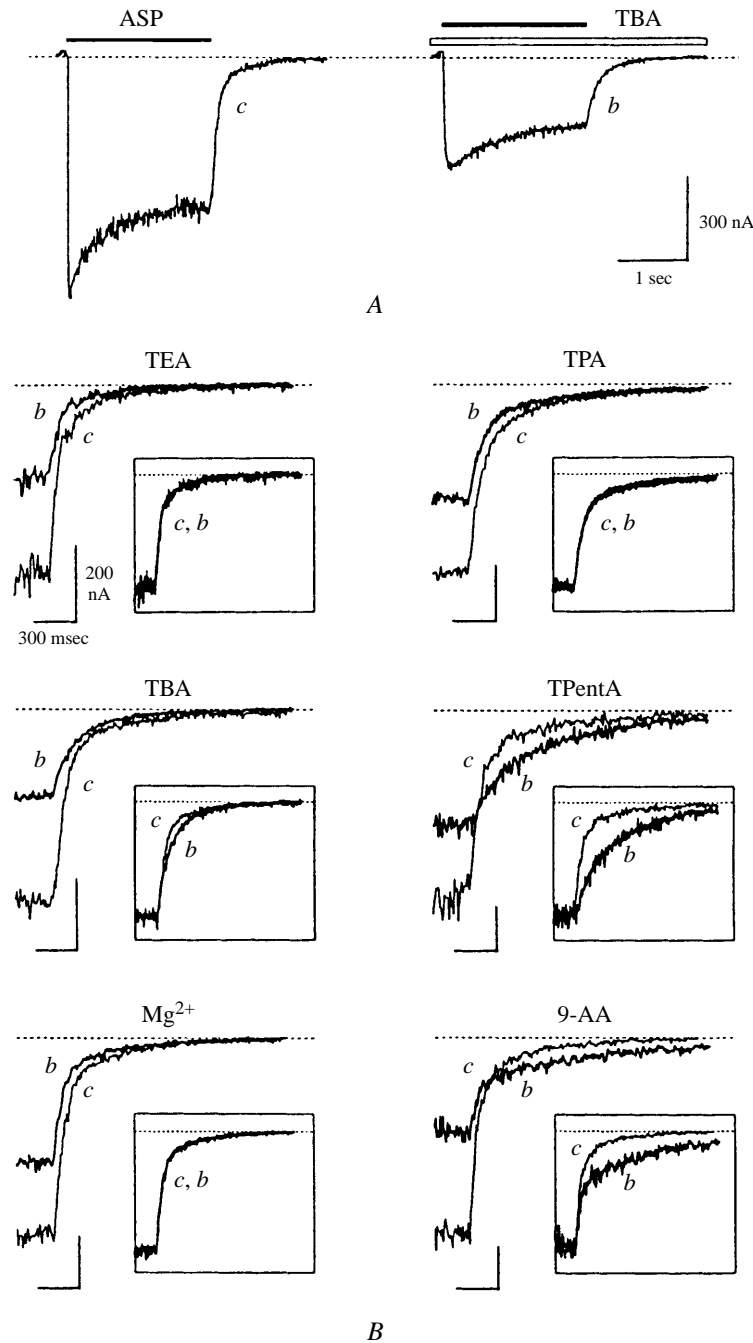


Fig. 4. The effect of exposure to agonist in the continuous presence of blocker (from [35] with additional data). A) Experimental scheme based on the example of 100 μ M aspartate (ASP) and 1 mM tetrabutylammonium (TBA); B) aftercurrents after the end of exposure to agonist in the continuous presence of tetraethylammonium (TEA, 2 mM), tetrapropylammonium (TPA, 0.6 mM), tetrabutylammonium (TBA, 1 mM), tetrapentylammonium (TPentA, 0.5 mM), Mg^{2+} (10 μ M), and 9-aminoacridine (9-AA, 10 μ M) (b) superimposed on control traces (c). Inserts show current curves for b and c with normalized stationary levels.

using tetrapentylammonium as an example, that $1 - (I_{BS}/I_{CS})$ increased with increases in the aspartate concentration. Apart from tetrapentylammonium, a positive agonist relationship was seen for 9-aminoacridine. In the cases of

tetraethylammonium, tetrapropylammonium, and Mg^{2+} , the degree of suppression of the stationary current was independent of the aspartate concentration, while for tetrabutylammonium the agonist relationship was negative (Fig. 3, B).

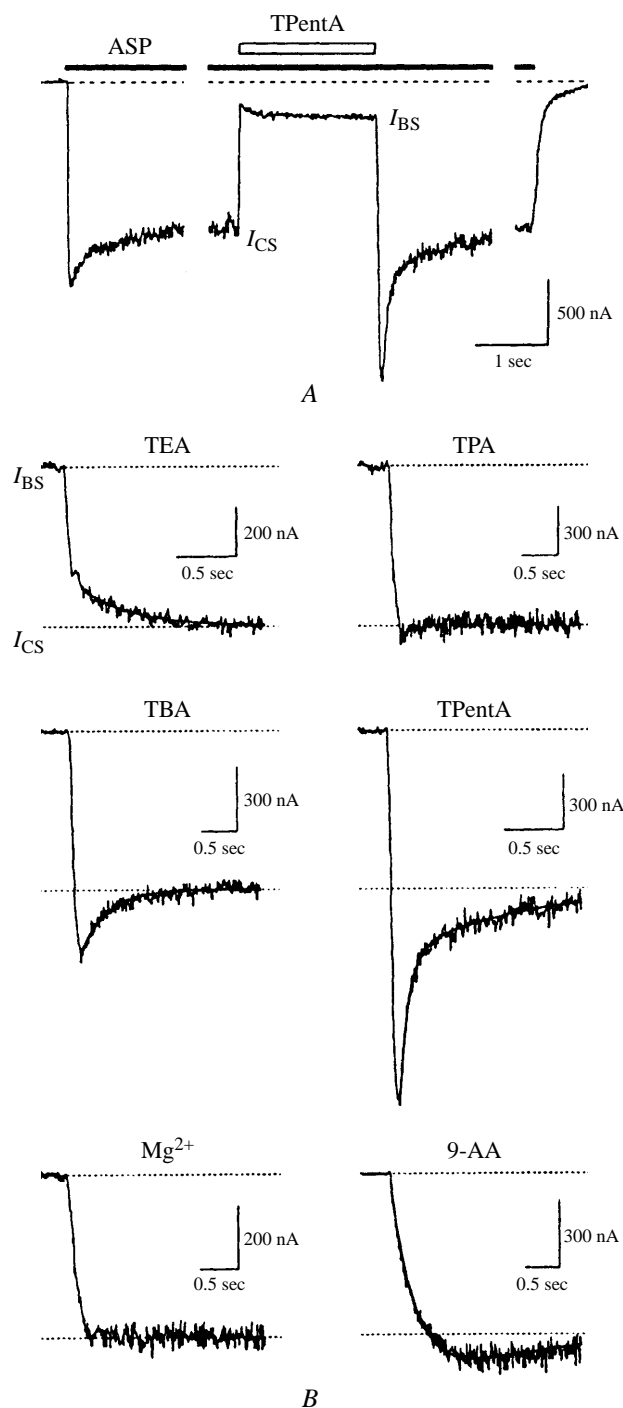


Fig. 5. Exposure to blockers in the continuous presence of agonist (from [35] with additional data). A) Experimental scheme based on the example of 2 mM tetrapentylammonium (TPentA) and 100 μ M aspartate (ASP); B) aftercurrents after the end of exposure to tetraethylammonium (TEA, 5 mM), tetrapropylammonium (TPA, 2 mM), tetrabutylammonium (TBA, 2 mM), tetrapentylammonium (TPentA, 2 mM), Mg^{2+} (100 μ M), and 9-aminoacridine (9-AA, 40 μ M) in the continuous presence of ASP (100 μ M).

When the blocker was constantly present in the solution washing the cell, there was no hook after the end of agonist exposure. The experiment is illustrated in Fig. 4, A, using 100 μ M aspartate and 1 mM tetrabutylammonium as an example. The aftercurrent kinetics after the end of aspartate exposure were very interesting. Superimpositions of aftercurrents in controls (*c*) and evoked by application of agonist in the constant presence of blocker (*b*) are shown in Fig. 4, B for different blockers. Curves *b* and *c* intersected in the cases of tetrapentylammonium and 9-aminoacridine, but not for the other blockers. The inserts in Fig. 4, B, where the stationary levels of current curves *c* and *b* are normalized, show that tetrapentylammonium and 9-aminoacridine produced strong delays in *b* as compared with *c*, this being very slight for tetrabutylammonium; normalized *c* and *b* curves coincided for Mg^{2+} , tetraethylammonium, and tetrapropylammonium.

Figure 5, A explains the experiment using blocker on a background of constant exposure to agonist solution, using tetrapentylammonium (2 mM) as an example. Blocker was used only after the aspartate-induced current had reached its stationary level (I_{CS}). After the end of tetrapentylammonium application, the current increased sharply to levels exceeding the stationary level of the control current (I_{CS}) and then gradually decayed to this level. The aftercurrent, which was greater than the stationary level in the control, subsequently demonstrated "overshoot." The overshoot decay in the case of tetrapentylammonium (Fig. 5, B) was well described by two exponents with time characteristics for the fast and slow components of $\tau_{fast} = 54 \pm 7$ msec and $\tau_{slow} = 596 \pm 85$ msec respectively ($n = 7$). Overshoot was also seen with tetrabutylammonium; when solution exchange was slow ($\tau_{wash} > 50$ msec), the descending phase of the overshoot contained one slow component ($\tau = 389 \pm 38$ msec, $n = 10$), while rapid solution exchange ($\tau_{wash} = 5\text{--}30$ msec) gave an overshoot decay which, as in the case of tetrapentylammonium, was well described by two exponents. In the cases of tetrapropylammonium and Mg^{2+} , overshoot, although present, was hardly detectable (Fig. 5, B). On average, the kinetics of current recovery after exposure to tetrapropylammonium and Mg^{2+} , in the continuous presence of aspartate, consisted of single rapid components reflecting the rate of solution exchange. Overshoot with 9-aminoacridine was only seen at high blocker concentrations, and its ascending phase was much slower ($\tau = 656 \pm 69$ msec at 40 μ M, $n = 7$) than in the cases of tetrabutylammonium and tetrapentylammonium. Overshoot did not develop at all with tetraethylammonium. In fact, the kinetics of recovery always contained a slow component, and the current was well described by two exponents with rapid- and slow-component time characteristics of $\tau_{fast} = 155 \pm 27$ msec and $\tau_{slow} = 2.04 \pm 0.34$ sec respectively; the amplitude of the fast component was $A_{fast} = 0.69 \pm 0.04$ ($n = 8$).

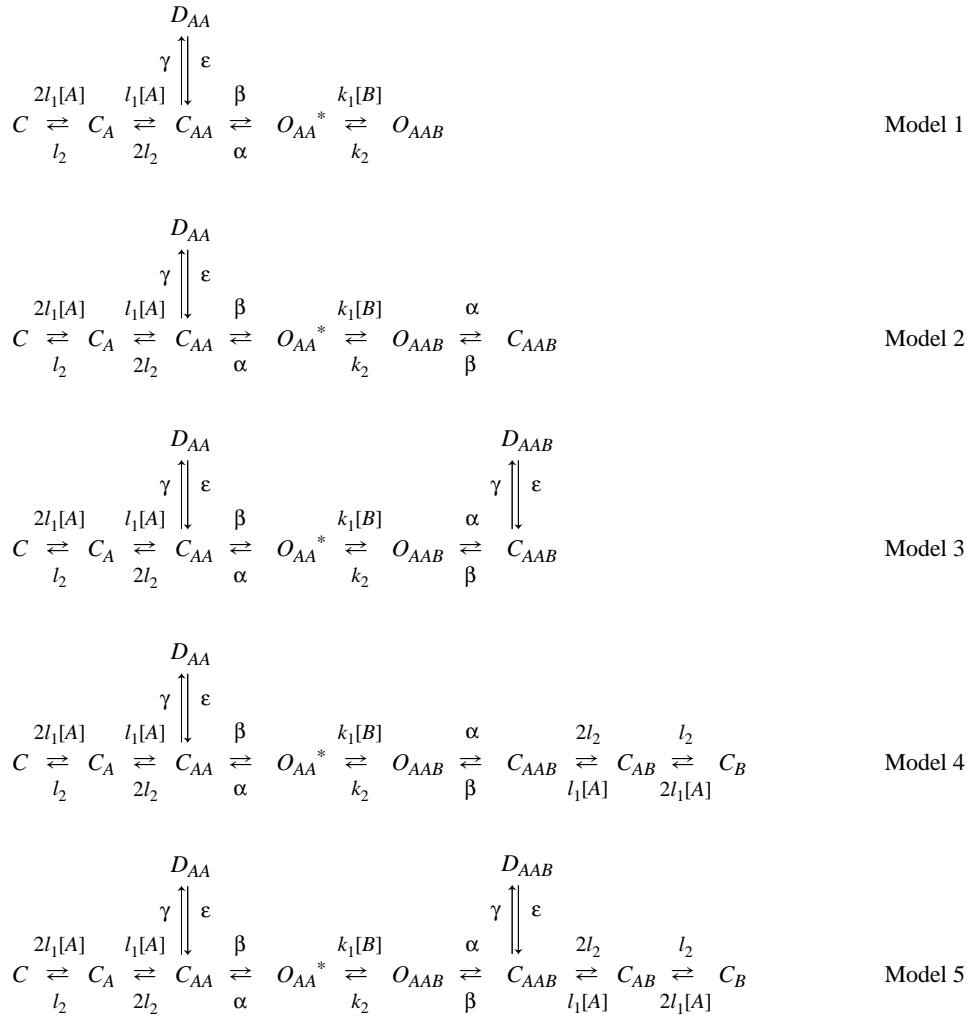


Fig. 6. Kinetic models describing different types of interaction between blocker and the NMDA channel (from [35]). C , D , and O indicate the channel in the closed, desensitized, and open states respectively. Indexes A , AA , and B designate the attachment of one molecule of agonist, two molecules of agonist, and one molecule of blocker respectively. Asterisks indicate the conducting state of the channel. $[A]$ and $[B]$ are the agonist and blocker concentrations respectively.

Kinetic Modeling. The effects of blockers on open channels were described by adding the blocked state to the standard kinetic model for activation of NMDA channels. Figure 6 shows five possible models obtained by sequential addition to the scheme of activation suggested by Lester and Jahr [26], the open blocked state (O_{AAB}), the closed blocked, agonist-non-bound (C_{AAB}), the desensitized blocked (D_{AAB}), and closed blocked states, in which agonist had already vacated the channel (C_{AB} , C_B).

The five models presented in Fig. 6 can be regarded as sequentially reduced models from the completely symmetrical model 5. The advantage of this set of models is that they are simple and allow the interactions of the blocker with the gating mechanism of the NMDA channel to be predicted. Model 1 describes the situation in which the blocker channel opening and, consequently, desensiti-

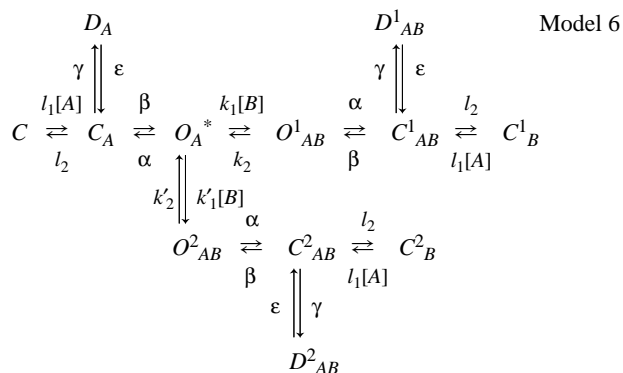
zation and agonist dissociation. The second model is based on the supposition that the channel can close with the blocker inside, but cannot undergo desensitization and the agonist-receptor complex cannot dissociate to such a stage that the channel is in the blocked state. The third model forbids only dissociation of the agonist, while the fourth only forbids desensitization. The last, fifth, model is symmetrical and forbids neither closure of the blocked channel, nor its desensitization, nor agonist dissociation. The values of kinetic constants, selected from our results and published data [7, 10, 16, 20, 33–35], were as follows: $l_1 = 2 \mu\text{M}^{-1}\text{sec}^{-1}$, $l_2 = 25 \text{ sec}^{-1}$, $\alpha = 200 \text{ sec}^{-1}$, $\beta = 10 \text{ sec}^{-1}$, $\gamma = 1.2 \text{ sec}^{-1}$, $\xi = 0.8 \text{ sec}^{-1}$, $k_1 = 3.5 \mu\text{M}^{-1}\text{sec}^{-1}$, and $k_2 = 1000 \text{ sec}^{-1}$. Testing of models 1–5 over wide ranges of parameters led to construction of the table of predictions (Table 2).

Comparison of the experimental data (Figs. 2–5) with the predictions of models 1–5 (Table 2) showed that the interaction of tetrapentylammonium with open NMDA channels was satisfactorily described by model 1.

The experimental data with Mg^{2+} and tetrapropylammonium were well described by symmetrical model 5. This model suggests that the blocker binds to the channel without preventing it from closing or undergoing desensitization or dissociation of agonist. The small deviations of the experimental data from the results of model experiments can be explained by the fact that Mg^{2+} and tetrapropylammonium can nonetheless have some effect on the desensitization of NMDA channels.

Comparison of the predictions of models 1–5 (Table 2) with the experimental data for tetraethylammonium suggests that the best model for describing its interaction is model 5. Two facts, however, indicate that model 5 cannot provide a complete description of the effects of tetraethylammonium: 1) the depth of the experimentally observed desensitization decay is significantly greater than predicted by the model [values of $(I_{BS}/I_{BO})/(I_{BS}/I_{CO})$ were significantly lower than predicted by model 5; compare Fig. 7, B and Fig. 2, C]; 2) the kinetics of recovery of the current after tetraethylammonium application ended, with aspartate present throughout, contained a slow component (Fig. 5, B), which is not predicted by model 5 (Fig. 7, E).

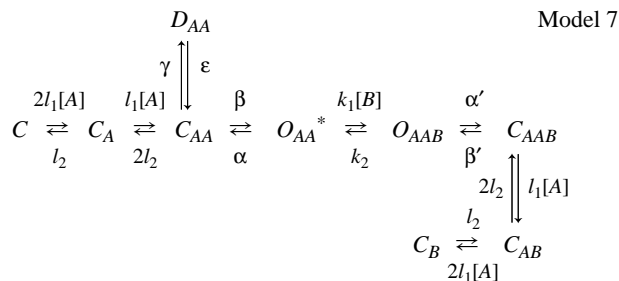
The simplest kinetic model providing a satisfactory description of the experimental data obtained with tetraethylammonium is the model with two binding sites for blocker, i.e., a fast site (1) and a slow site (2).



The binding and dissociation constants for site 2 were taken to be 250 times smaller than the corresponding constants for site 1: $k_2' = k_2/250 = 4 \text{ sec}^{-1}$ and $k_1' = k_1/250 = 0.014 \mu\text{M}^{-1}\text{sec}^{-1}$. Analysis of the results of modeling may indicate that the NMDA channel contains two blocking sites for the binding of tetraethylammonium, which cannot be occupied simultaneously by two blocker molecules, and that binding with site 1, which has rapid binding and dissociation kinetics, does not prevent binding and desensitization of the NMDA channel and dissociation of agonist.

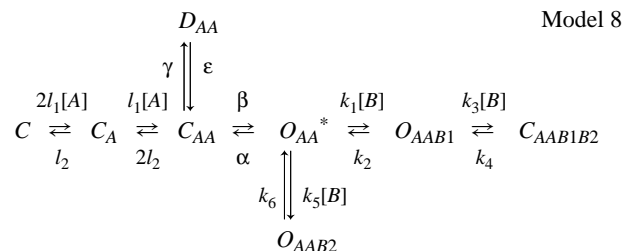
Returning to Table 2, it seems that the best model for describing the effects of tetraethylammonium is model 4.

The following points, however, suggest that model 4 cannot describe all its effects: 1) the hook exceeds the stationary level of the control current (Fig. 2, A); 2) there is a delay in aftercurrent decay kinetics in the continuous presence of blocker in solution, as compared with controls (Fig. 4, B); and 3) there is a rapid phase in the overshoot decay on rapid exchange of solutions. The simplest model satisfactorily describing the experimental data is model 4 with an alteration in the $O_{AAB}-C_{AAB}$ transition.



Kinetic analysis showed that correspondence with the experimental data needed tetraethylammonium to increase the maximum probability of opening of blocked channels [$P_0' = \beta' / (\alpha' + \beta')$] as compared with the corresponding value for the unblocked channel [$P_0 = \beta / (\alpha + \beta)$]. There are two possible ways to do this: to alter the closing constant (α') or to alter the opening constant (β'). Decreases in α' would suggest that the blocker prevents closure of channels, while increases in β' would suggest that the blocker, having entered the channel, facilitates its opening. Both possibilities produce qualitatively identical results. Figure 7 shows the results of model experiments addressing the possibility that the blocker hinders channel closure by a factor of 20 ($\alpha' = \alpha/20 = 10 \text{ sec}^{-1}$, $\beta' = \beta$).

The simplest kinetic model describing the effects of 9-aminoacridine supposes that the blocker prevents closure of the channel and thus prevents desensitization and dissociation of agonist [10, 15, 33], and also assumes two binding sites for 9-aminoacridine in the NMDA channel and the possibility that these can simultaneously be occupied by two different blocker molecules [33].



This model supposes that the blocker bound with either of the sites prevents both closure of the channel and its desensitization and dissociation of agonist. Figure 7 shows the predictions of model 8 with the following values of the

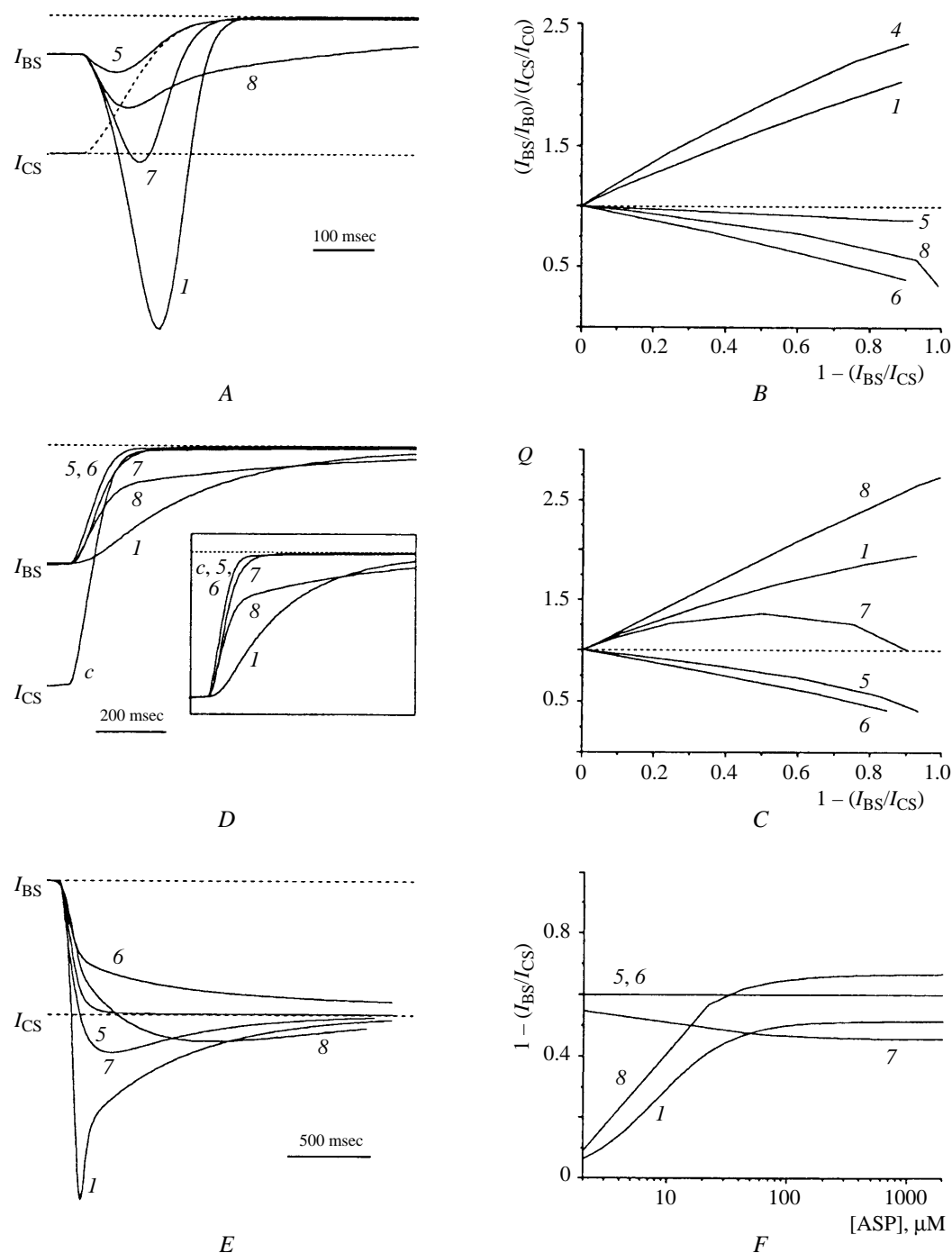


Fig. 7. Predictions of models describing the actions of blockers (identified by numbers). A) Aftercurrents appearing after the end of simultaneously application of blocker and agonist continuous lines) superimposed on control traces (dotted lines); B, C) relationships of control-normalized ratios of stationary current to peak current $[(I_{BS}/I_{BO})/(I_{CS}/I_{CO})]$ (B) and control-normalized charge transfer during the aftercurrent (Q) (C) with the extent of suppression of the stationary current $(1 - (I_{BS}/I_{CS}))$; D) aftercurrents appearing after the end of application of agonist in the continuous presence of blocker superimposed on control traces (c). The insert shows current curves with normalized stationary levels; E) aftercurrents appearing after the end of exposure to blocker in the continuous presence of agonist; F) relationship between the extent of suppression of the stationary current and the agonist concentration.

TABLE 2. Predictions of Models 1–5 (from [35] with additional data)

Model	Criteria for model 5		Criteria for desensitization		Criteria for channel closure	Criteria for agonist dissociation		
	Probability of $I_P > I_{CS}$	Intersection during coapplication ¹	$(I_{BS}/I_{B0}) / (I_{CS}/I_{C0})$	Overshoot ²	Rapid phase of overshoot ³	Q^4	Agonist dependence ⁵	Intersection in the presence of blocker ⁶
1	+	+	>1	+	+	>1	Increasing	+
2	+	+	>1	+	–	>1	Increasing	+
3	+	+	<1	–	–	>1	Increasing	+
4	+	+	>1	+	–	<1	Decreasing	–
5	–	–	<1	–	–	<1	Constant	–

Notes. ¹Intersection (on superimposition of traces) of the aftercurrent in controls and the current after coapplication of agonist and blocker. ²Presence of overshoot of the aftercurrent in the presence of agonist. ³Probability of the appearance of a rapid component in the overshoot decay phase. ⁴Magnitude of control-normalized charge transfer during the aftercurrent. ⁵Agonist dependence of the extent of suppression of the stationary current. ⁶Intersection (on superimposition of traces) of the control aftercurrent and the current after the end of application of agonist in the continuous presence of blocker.

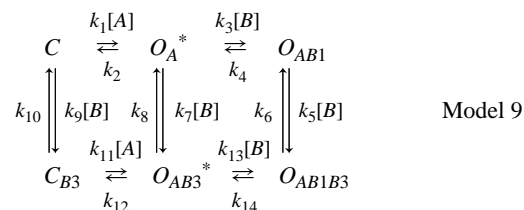
kinetic constants: $k_1 = 29 \mu\text{M}^{-1}\text{sec}^{-1}$, $k_2 = 1000 \text{ sec}^{-1}$, $k_3 = 0.74 \mu\text{M}^{-1}\text{sec}^{-1}$, $k_4 = 1.54 \text{ sec}^{-1}$, $k_5 = 0.054 \mu\text{M}^{-1}\text{sec}^{-1}$, and $k_6 = 0.47 \text{ sec}^{-1}$.

Thus, description of the kinetics and stationary characteristics of NMDA channel blockade by different substances needed different kinetic models. This suggests that the mechanisms of action of these blockers are different. The first point is that models based on different actions for blockers on the processes of channel closure, channel desensitization, and dissociation of agonist, with identical microscopic equilibrium dissociation constants ($K_d = k_2/k_1$) predict different apparent blocker affinities for channels (IC_{50}). This is an important question, as the microscopic dissociation constant and the half-blocking concentration are often the same, which in turn leads to incorrect interpretation of the data and erroneous comparative analysis.

It follows that the apparent affinity of tetraalkylammonium compounds [$(1/\text{IC}_{50})$, $(1/K_{0.5}(0))$] depend not only on hydrophobic and steric factors (which influence the microscopic K_d), but also on interactions with the gating mechanism [affecting the difference between IC_{50} values ($K_{0.5}(0)$ and K_d)]. The ratio of K_d and IC_{50} depends on the probability of channel opening (P_0), on the number of desensitized channels, and also on the concentration of agonist. For model 5, IC_{50}/K_d is always unity. For the other models, this ratio is always greater than unity. Thus, with $P_0 = 0.048$, $\gamma/\varepsilon = 1.5$ and an asparagine concentration of $2.5 \mu\text{M}$, model 1 gives $\text{IC}_{50}/K_d = 1000$.

Screening Effect. A second possible source of differences between the microscopic K_d and the half-blocking concentration IC_{50} is the mechanism of “screening.” Screening means the existence of a non-blocked binding site, such that attachment of one blocker molecule to this site hinders the binding of another blocker molecule to the blocked site (Fig. 8, C). The blocked binding site (1) is deep within the channel pore, while the screening site (3) is in the

wide part of the extracellular vestibule. The screening effect is manifest as a deviation in the value of the Hill coefficient for the relationship between concentration and the extent of suppression of the stationary current from unity, i.e., the value predicted by all eight of the kinetic models analyzed above. Thus, the greater the binding of one blocker molecule to the screening binding site hinders binding of a second blocker molecule to the blocked site, the smaller is the Hill coefficient. It is logical to suppose that the larger the blocker molecule, the greater the screening effect it would have. The significant decrease in the Hill coefficient with blocker molecule size seen for tetraalkylammonium compounds (Table 3) agrees with this hypothesis. The simplest kinetic model describing the screening effect is



The applicability of the screening model hypothesis was assessed by testing model 9 with $k_1 = k_{11} = 4 \text{ sec}^{-1}\mu\text{M}^{-1}$, $k_2 = k_{12} = 50 \text{ sec}^{-1}$, $k_3 = k_5 = k_7 = k_9 = 100 \text{ sec}^{-1}[\text{B}]^{-1}$, and $k_4 = k_6 = k_8 = k_{10} = k_{14} = 100 \text{ sec}^{-1}$. The rate constant k_{13} was varied. Calculated curves showing the relationship between the extent of suppression of the stationary current and blocker concentration, expressed as $K_d = k_4/k_3$ at different k_{13} values, are shown in Fig. 8, B. When constant k_{13} was less than k_3 (binding of one blocker molecule to the screening site hinders binding of another blocker molecule to the blocked site), the relationship between the extent of suppression of the stationary current and the blocker concentration was less steep and the Hill coefficient was less than unity (Fig. 8, C). The ratio IC_{50}/K_d increased in these conditions and was greater

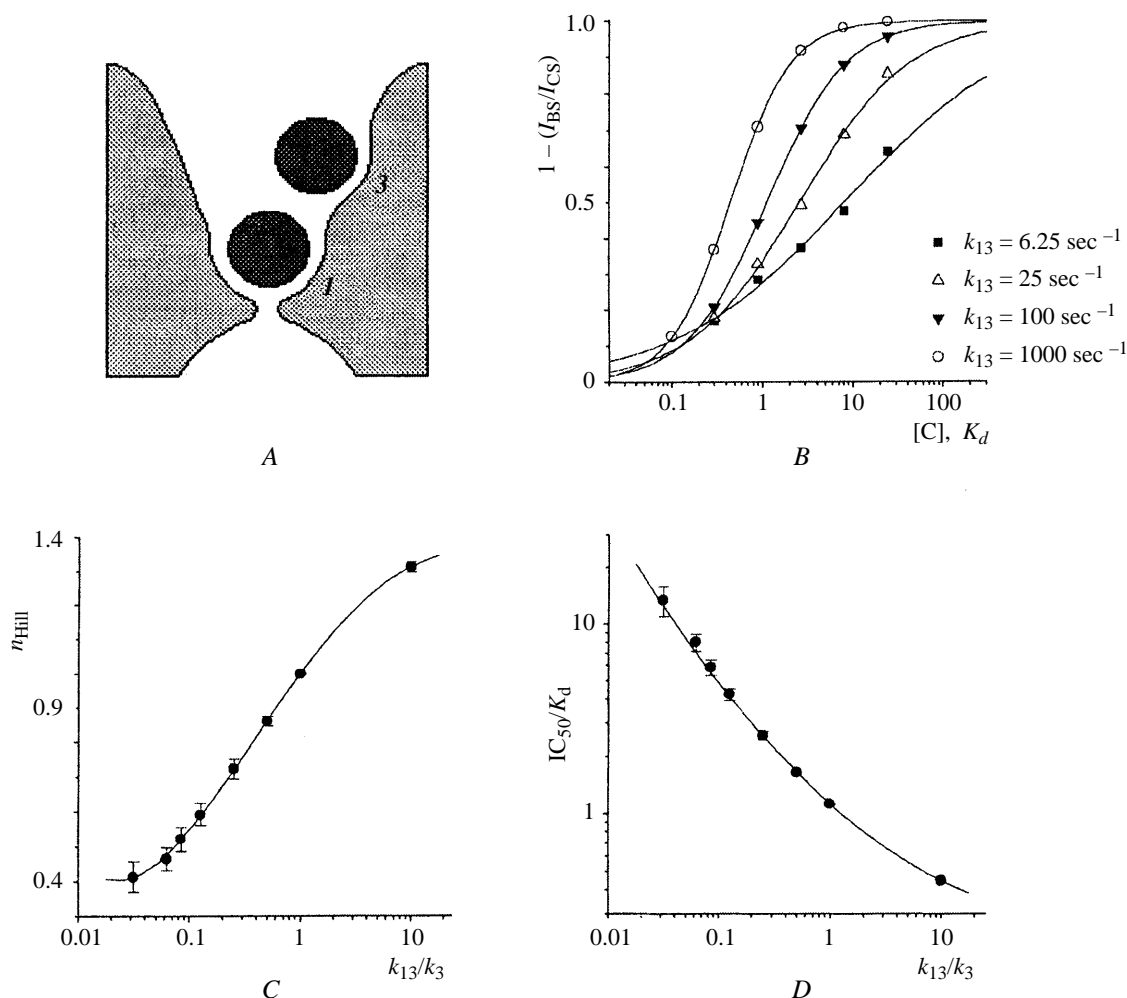


Fig. 8. The "screening" hypothesis. A) Diagram showing the screening hypothesis. The blocker binding sites (1 is the blocking site and 3 is the screening site) are located in the extracellular vestibule of the channel. Circles identify blocker molecules. The narrow part of the channel is just below site 1, the selective filter; B) relationship between the extent of suppression of the stationary current predicted by model 9 at different values of constant k_{13} . Curves show fitting to the equation; C) relationship between the Hill coefficient and the ratio k_{13}/k_3 ; D) relationship between ratio IC_{50}/K_d and k_{13}/k_3 .

than unity (Fig. 8, D). Conversely, when k_{13} was greater than k_3 (binding of one blocker molecule to the screening site facilitated binding of another blocker molecule to the blocked site), the plot showing suppression of the stationary current was steeper and the Hill coefficient was greater than 1 (Fig. 8, C), while IC_{50}/K_d decreased (Fig. 8, D).

The Roles of Hydrophobicity and the Size of Tetraalkylammonium Compounds in Their Binding to NMDA Channels. Having found the coefficients of increase of IC_{50} as compared with K_d , due to the interaction with the gating mechanism (k_g), and the screening mechanism (k_s), values of $K_{0.5}(0)$ can be used to estimate microscopic equilibrium dissociation constants at $E_h = 0 \text{ mV}$: $k_d(0)_{\text{micro}} = K_{0.5}(0)/k_g/k_s$. Calculated values of k_g , k_s , and $k_d(0)_{\text{micro}}$ for tetraalkylammonium compounds are shown in Table 3.

The change in the free binding energy of tetraalkylammonium compounds, per mole of alkyl groups, with NMDA channels, calculated according to

$$\delta G(=CH_2) = -(1/4)RT\delta[\ln(K_d(0)_{\text{micro}})],$$

gave $\delta G(=CH_2)$ values of 318 cal/mole going from tetraethylammonium to tetrapropylammonium, 569 cal/mole going from tetrapropylammonium to tetrabutylammonium, and 555 cal/mole going from tetrabutylammonium to tetrapentylammonium. Linear fitting of $\ln[K_d(0)_{\text{micro}}]$ for all tetraalkylammonium compounds gave $\delta G(=CH_2) = 489 \pm 42 \text{ cal/mole}$ (Fig. 9). This value is half the theoretical change in the free energy of one mole of $=CH_2=$ groups (1000 cal/mole) for transfer from an aqueous environment to a hydrophobic environment [23]. Con-

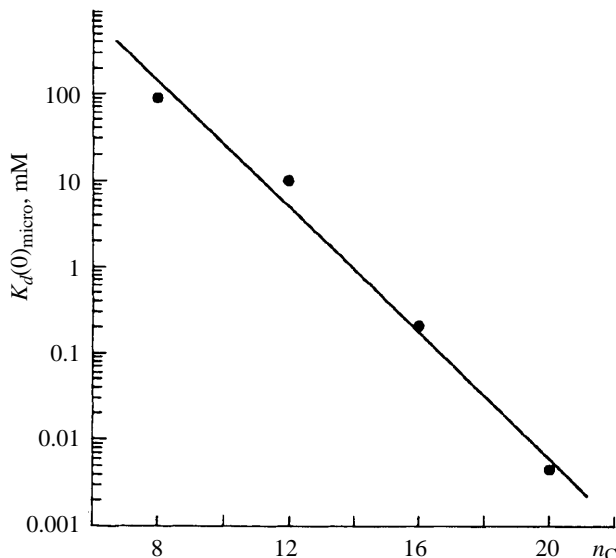


Fig. 9. Relationship between $K_d(0)_{\text{micro}}$ and the number of carbon atoms (n_C) in tetraalkylammonium compounds.

TABLE 3. Values of k_g , n_{Hill} , k_s , and $K_d(0)_{\text{micro}}$ for Tetraalkylammonium Compounds

Substance	k_g	n_{Hill}	k_s	$K_d(0)_{\text{micro}}$, mM
Tetraethylammonium	1	1.22 ± 0.08	0.7	88.9 ± 8.6
Tetrapropylammonium	1	1.06 ± 0.04	1	10.0 ± 1.5
Tetrabutylammonium	16.4	0.88 ± 0.09	1.63	0.20 ± 0.01
Tetrapentylammonium	49	0.65 ± 0.02	8.5	0.0044 ± 0.0003

sidering that the positive charge of the nitrogen atom in all tetraalkylammonium compounds is distributed over the alkyl chain and that the binding regions of these compounds cannot be regarded as ideal non-polar hydrophobic environments, the transfer energy of one mole of $=\text{CH}_2=$ groups must be less than 1000 cal/mole. Thus, hydrophobic interactions play a large role in the binding of tetraalkylammonium compounds with NMDA channels and it can be suggested that at least half the $=\text{CH}_2=$ groups of these compounds form hydrophobic bonds when blocking channels. Contradicting the conclusions of a previous study [2], we came to the conclusion that the absence of any significant decrease in $\delta G(=\text{CH}_2=)$ with increases in the length of the alkyl chain is evidence that the size of the tetraalkylammonium compounds has no effect on their ability to form hydrophobic bonds in NMDA channels.

A Model for the Gating Mechanism of NMDA Channels. The difference in the mechanisms of action of blockers is apparent mainly in their effects on channel closure, channel desensitization, and agonist dissociation. Some blockers prevent closure of NMDA channels (tetrapentylammonium), while others (tetrabutylammoni-

um) only decrease the probability that the blocked channel will be in the closed state and, finally, a third group have no effect on closure (Mg^{2+} , tetraethylammonium, and tetrapropylammonium). This is evidence for the existence of activatory gates in NMDA channels, on which blockers can act in different ways. The fact that some blockers prevent desensitization of NMDA channels (tetrapentylammonium, tetrabutylammonium, and 9-aminoacridine), while others only have partial effects on NMDA channels (Mg^{2+} and tetrapropylammonium), and, finally, a third group has no effect (tetraethylammonium) suggests that the NMDA channel contains some structure responsible for its desensitization and on which different blockers can act in different ways. The existence of a blocker which does not prevent closure of NMDA channels but does prevent desensitization (tetrabutylammonium) shows that the activatory gate of the NMDA channel and the structure responsible for channel desensitization are different from each other. Since all the study substances enter the pore and block the channel, this structure is most likely to be located in the transmembrane pore-forming fragments of the amino-acid sequence of the NMDA channel.

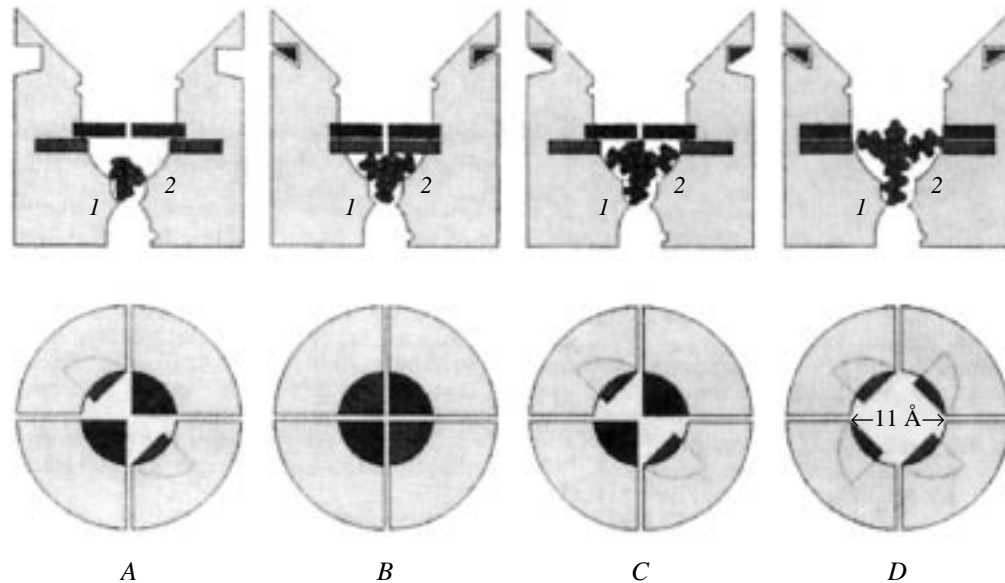


Fig. 10. Explanation of the hypothesis that NMDA channels contain activatory and desensitizing gates, which are different from each other (from [35]). The activatory gates are shown darker than the desensitizing gates and are located closer to the extracellular surface of the membrane. Triangles show agonist molecules. Hemispheres in the channel walls are binding sites for penetrating cations. 1, 2) Blocker binding sites. The upper row shows side views, and the lower row shows views from above. A) An NMDA channel with bound tetraethylammonium in the closed agonist-non-bound blocked state (C_B); B) a channel with bound tetrapropylammonium in the desensitized blocked state (D_{AAB}); C) a channel with bound tetrabutylammonium in the closed agonist-bound blocked state (C_{AAB}); D) a channel with bound tetrapentylammonium in the open blocked state (O_{AAB}).

The molecules of blockers which prevent closure or desensitization of the NMDA channel are large in size. Blockers which do not prevent but can hinder these processes are smaller, and blockers which hinder neither closure nor desensitization are the smallest. This is evidence for the suggestion that blocker molecule size plays the key role in the interactions of blockers with the gating structures of the NMDA channel [2]. The fact that the value of δ for small-size blockers is significantly greater than δ for large blockers (Table 1) is indirect evidence that the former penetrate more deeply into the channel pore than the latter.

According to current concepts, the NMDA channel is a pore with a small intracellular vestibule and a large extracellular vestibule containing a narrowing of length about 6 Å and a diameter of 6.4 Å; the vestibules are separated by a selective filter with a cross-section of 22–26 Å [37, 40]. Figure 10 shows part of the pore of the NMDA channel, containing two blocking regions and binding sites for cations which penetrate the pore. The latter are most likely to be located in the upper part of the ion pore (the extracellular vestibule), because the binding of penetrating cations to them is independent of membrane potential [3, 5]. It is very likely that one or several binding sites for penetrating cations are at the same time screening binding sites (Fig. 8). The structure responsible for opening and closing of the NMDA channel is shown in Fig. 10 as an activatory gate separated from the selective filter by a distance no greater

than the length of the extended IEM-1754 molecule (17 Å), whose terminal ammonium group attaches to site 1 at a membrane potential of –90 mV, while the adamantane head prevents closure of the activatory gates [4, 6, 21].

The structure responsible for desensitization of the NMDA channel is also shown in Fig. 10 as gates. Thus, blockers preventing channel closure or desensitization prevent closure of the corresponding gates. The difference in the depths of the activatory and desensitizing channel gates is determined mainly by the difference in the sizes of tetrapentylammonium and tetrabutylammonium. Since this is small (1–2 Å), it is logical to suppose that the activatory and desensitizing gates are formed from transmembrane fragments of different subunits of the NMDA channel. This suggestion is shown in diagram form as views of the channel from above (Fig. 10, lower row).

There is an alternative suggestion, that only the activatory gates are within the channel pore, while the structure responsible for desensitization is outside the pore-forming channel walls. This structure can be illustrated as “bolts,” which completely lock the closed activatory gates, converting the channel into the non-conducting desensitized state.

Regardless of the actual structure of the “desensitizing gates” of the NMDA channel, the diameter of the channel pore at the activatory gate site has to be taken as essentially the same as the size of the tetrapentylammonium molecule (11 Å), calculated as the mean of the two minimum sizes of

the smallest box containing the tetrapentylammonium molecule (HyperChem) (and which is equal to the cross-sectional size of the 9-aminoacridine molecule). This is in good agreement with data obtained by Koshelev and Khodorov [2], who came to the conclusion that only those blockers whose maximum molecular size is greater than the critical size of the window, 11 Å, have the ability to immobilize the open configuration of the channel. In this case, if the desensitizing mechanism shown in Fig. 10 is correct, the diameter of the channel pore in the region of the desensitizing gates is essentially equal to the size of the tetrabutylammonium ammonium molecule (10 Å).

Thus, the present results lead to the conclusion that blockers are useful tools for studying the functional architecture of receptor-controlled channels in neuron membranes.

This study was supported by the Russian Fund for Basic Research (Grant Nos. 96-15-97866 and 99-04-48770) and a grant from the Physiological Society of Great Britain.

REFERENCES

1. S. G. Koshelev and B. I. Khodorov, "Tetraethylammonium and tetrabutylammonium as tools for studies of NMDA channels in neuron membranes," *Biol. Membrany*, **9**, 1365–1369 (1992).
2. S. G. Koshelev and B. I. Khodorov, "Tetrabutylammonium, tacrine, and 9-aminoacridine, which block open NMDA channels, prevent channel closure and desensitization," *Biol. Membrany*, **12**, 89–104 (1995).
3. S. M. Antonov, V. E. Gmiro, and J. W. Johnson, "Binding sites for permeant ions in the channel of NMDA receptors and their effects on channel block," *Nat. Neurosci.*, **1**, 451–456 (1998).
4. S. M. Antonov and J. W. Johnson, "Voltage-dependent interaction of open-channel blocking molecules with gating of NMDA receptors in rat cortical neurons," *J. Physiol.*, **493**, 425–445 (1996).
5. S. M. Antonov and J. W. Johnson, "Permeant ion regulation of N-methyl-D-aspartate receptor channel block by Mg^{2+} ," *Proc. Natl. Acad. Sci. USA*, **96**, 14571–14576 (1999).
6. S. M. Antonov, J. W. Johnson, N. Y. Lukomskaya, N. N. Potapyeva, V. E. Gmiro, and L. G. Magazanik, "Novel adamantane derivatives act as blockers of open ligand-gated channels and as anticonvulsants," *Mol. Pharmacol.*, **47**, 558–567 (1995).
7. P. Ascher, P. Bregestovski, and L. Nowak, "NMDA-activated channels of mouse central neurons in magnesium-free solutions," *J. Physiol.*, **399**, 207–226 (1988).
8. F. Asztely and B. Gustafsson, "Ionotropic glutamate receptors: Their role in the expression of hippocampal synaptic plasticity," *Mol. Neurobiol.*, **12**, 1–11 (1996).
9. M. Benveniste and M. L. Mayer, "Kinetic analysis of antagonist action at N-methyl-D-aspartic acid receptors. Two binding sites each for glutamate and glycine," *Biophys. J.*, **59**, 560–573 (1991).
10. M. Benveniste and M. L. Mayer, "Trapping of glutamate and glycine during open channel block of rat hippocampal neuron NMDA receptors by 9-aminoacridine," *J. Physiol.*, **483**, 367–384 (1995).
11. M. Benveniste, J.-M. Mienville, E. Sernafor, and M. L. Mayer, "Concentration-jump experimental with NMDA antagonists in mouse cultured hippocampal neurons," *J. Neurophysiol.*, **63**, 1373–1384 (1990).
12. T. V. Bliss and G. L. Collingridge, "A synaptic model of memory: long-term potentiation in the hippocampus," *Nature*, **361**, 31–39 (1993).
13. H. T. Cline, E. A. Debski, and M. Constantine-Paton, "The role of NMDA receptor in the development of the frog visual system," *Adv. Exp. Med. Biol.*, **268**, 197–203 (1990).
14. M. Constantine-Paton, "NMDA receptor as a mediator of activity-dependent synaptogenesis in the developing brain," *Cold. Spring Harb. Symp. Quant. Biol.*, **55**, 431–443 (1990).
15. A. C. S. Costa and E. X. Albuquerque, "Dynamics of the actions of tetrahydro-9-aminoacridine and 9-aminoacridine on glutamatergic currents. Concentration-jump studies in cultured rat hippocampal neurons," *J. Pharmacol. Exp. Ther.*, **268**, 503–514 (1994).
16. S. G. Cull-Candy and M. M. Usowich, "On the multiple-conductance single channels activated by excitatory amino acids in large cerebellar neurones of the rat," *J. Physiol.*, **415**, 555–582 (1989).
17. W. Danysz and C. G. Parsons, "Glycine and N-methyl-D-aspartate receptors. Physiological significance and possible therapeutic application," *Pharmacol. Rev.*, **50**, 597–664 (1998).
18. W. Danysz, C. G. Parsons, I. Breskink, and G. Quack, "Glutamate in CNS disorders," *Drug News Perspect.*, **8**, 261–277 (1995).
19. R. Dingledine, K. Borges, D. Bowie, and S. F. Traynelis, "The glutamate receptor ion channels," *Pharmacol. Rev.*, **51**, 7–61 (1999).
20. C. E. Jahr and C. F. Stevens, "A quantitative description of NMDA receptor channel kinetic behavior," *J. Neurosci.*, **10**, 1830–1837 (1990).
21. J. W. Johnson, S. M. Antonov, T. S. Blanpied, and Y. Li-Smerin, "Channel block of NMDA receptor," in: *Excitatory Amino Acids and Synaptic Transmission*, H. V. Wheal (ed.), Academic Press Inc., London (1997), pp. 99–113.
22. J. W. Johnson and P. Ascher, "Glycine potentiates the NMDA response in cultured mouse brain neurons," *Nature*, **325**, 529–531 (1987).
23. W. Kauzmann, "Some factors in the interpretation of protein denaturation," *Adv. Protein Chem.*, **14**, 1–63 (1959).
24. H. Komuro and P. Pakic, "Modulation of neuronal migration by NMDA receptors," *Science*, **260**, 95–97 (1993).
25. R. Lester, J. D. Clements, G. L. Westbrook, and C. E. Jahr, "Channel kinetics determine the time course of NMDA receptor-mediated synaptic currents," *Nature*, **346**, 565–567 (1990).
26. R. A. J. Lester and C. E. Jahr, "NMDA channel behaviour depends on agonist affinity," *J. Neurosci.*, **12**, 635–643 (1992).
27. S. A. Lipton, "Prospects for clinically tolerated NMDA antagonists: open-channel blockers and alternative redox states of nitric oxide," *TINS*, **16**, 527–532 (1993).
28. A. B. MacDermott, M. L. Mayer, G. L. Westbrook, S. J. Smith, and J. L. Baker, "NMDA receptor activation increases cytoplasmic calcium concentration in cultured spinal cord neurones," *Nature*, **321**, 519–522 (1986).
29. S. Maren and M. Baudry, "Properties and mechanisms of long-term synaptic plasticity in the mammalian brain: relationships to learning and memory," *Neurobiol. Learn. Mem.*, **63**, 1–18 (1995).
30. L. Nowak, P. Bregestovski, P. Ascher, A. Herbert, and A. Prochiantz, "Magnesium gates glutamate-activated channels in mouse central neurones," *Nature*, **307**, 462–465 (1984).
31. C. G. Parsons, W. Danysz, and G. Quack, "Glutamate in CNS disorders as a target for drug development: an update," *Drug News Perspect.*, **11**, 523–569 (1998).
32. C. G. Parsons, W. Danysz, and G. Quack, "Memantine is a clinically well tolerated N-methyl-D-aspartate (NMDA) receptor antagonist – a review of preclinical data," *Neuropharmacology*, **38**, 735–767 (1999).
33. A. I. Sobolevsky, "Two-component blocking kinetics of open NMDA channels by organic cations," *Biochim. Biophys. Acta*, **1416**, 69–91 (1999).
34. A. Sobolevsky and S. Koshelev, "Two blocking sites of amino-adamantane derivatives in open N-methyl-D-aspartate channels," *Biophys. J.*, **74**, 1305–1319 (1998).

35. A. I. Sobolevsky, S. G. Koshelev, and B. I. Khodorov, "Probing of NMDA channels with fast blockers," *J. Neurosci.*, **19**, 10611–10626 (1999).
36. H. G. Traven, L. Brodin, A. Lansner, O. Ekeberg, P. Wallens, and S. Grillner, "Computer simulations of NMDA and non-NMDA receptor-mediated synaptic drive: sensory and supraspinal modulation of neurons and small networks," *J. Neurophysiol.*, **70**, 695–709 (1993).
37. A. Villarroel, N. Bernashev, and B. Sakmann, "Dimensions of the narrow portion of a recombinant NMDA receptor channel," *Biophys. J.*, **68**, 866–875 (1995).
38. V. S. Vorobjev, "Vibrodisssection of sliced mammalian nervous tissue," *J. Neurosci. Methods*, **38**, 145–150 (1991).
39. A. M. Woodhull, "Ionic blockage of sodium channels in nerve," *J. Gen. Physiol.*, **61**, 687–708 (1973).
40. M. M. Zarei and J. A. Dani, "Structural basis for explaining open-channel blockade of the NMDA receptor," *J. Neurosci.*, **15**, 1446–1454 (1995).